Article

How Sensitive Morphological Parameters Influence on the PM$_{2.5}$ Diffusion: An Empirical Study of Two Neighborhoods in Central Beijing

Peihao Zhang [1], Haomiao Cheng [1,*] , Zhiwen Jiang [2] and Fanding Xiang [1]

[1] College of Architecture and Urban Planning, Beijing University of Technology, Beijing 100121, China; zhangpeih@outlook.com (P.Z.); xiangfandel@outlook.com (F.X.)
[2] Key Laboratory of Beijing on Regional Air Pollution Control, Faculty of Environment and Life, Beijing University of Technology, Beijing 100121, China; jiangzw@foxmail.com
[*] Correspondence: chenghaomiao@bjut.edu.cn

Abstract: Air quality is highly related to the health of a human being. Urban morphology has a significant influence on air quality; however, the specific relationship between urban morphology characteristics and air quality at the neighborhood scale has yet to be investigated, especially the vegetation effect on PM$_{2.5}$ concentration and diffusion. The relevant morphological parameters based on the affected pathways of urban morphology on air quality were selected, and the sensitivity degree and laws of the selected morphological parameters to PM$_{2.5}$ were quantified by numerical simulation, bivariate correlation analysis, and regression analysis. The results showed that Building Density (BD), Block Envelope Degree (BED), Average Building Volume (ABV), Average Building Floors (ABF), Standard Deviation of Building Height (SDH) and Greenbelt Coverage Rate (GCR) were Sensitive Morphological Parameters (SMPs). A positive and cosine curve trend of BD and BED with PM$_{2.5}$ was observed. GCR was significant to dust retention along with vertical canopy height. When ABV = 40,000 m^3 and ABF = 20F, the lowest PM$_{2.5}$ concentration was examined, while increased SDH could promote airflow and enhance the capacity of PM$_{2.5}$ diffusion. Finally, morphology-optimization strategies were proposed at the neighborhood scale: (1) Decreasing the BED along the street; (2) considering the species of vegetation with the appropriate height and increasing the GCR; (3) increasing the ABF of neighborhoods appropriately while controlling the ABV and distinguishing the internal SDH of neighborhoods. The study could apply the scientific basis for the planning and design of healthy and livable cities.

Keywords: sensitive morphological parameters; PM$_{2.5}$; CFD; neighborhoods; Beijing

1. Introduction

Rapid urbanization has resulted in air pollution issues that had a negative impact on many sectors of human lives. According to the Beijing State of the Environment Bulletin 2020 [1], the number of days that met air quality standards in 2020 was 276 days, accounting for 75.4%. Although the overall air quality has improved compared to the previous period, the distribution of pollution still showed north–south differences, and the concentration of pollutants such as PM$_{2.5}$ and PM10 in ecological zones in the north and northwest is significantly lower than that in the southern high-density built-up areas and high-density population areas, which showed a "Low-Northwest while High-Southeast" situation. As urban planning became a more essential component of the development of livable cities, how to enhance air quality by optimizing urban morphology evolved into a focus of investigation in relevant disciplines [2,3].

Based on the foregoing, studies on urban morphology and air quality were steadily established [4]. Studies mainly involve two scales: regional-urban [5] and neighborhoods [6]. At the regional-urban scale, most scholars had focused on exploring the intrinsic effects

of different urban morphological features on air quality. Research elements included physical spatial characteristics such as city size and urban shape, [7] vegetation cover [8], and non-physical characteristics such as population density and employment density [9]. In addition, studies have also been conducted to analyze the correlation between urban morphology and air quality from a spatial and temporal perspective [10].

At the neighborhood scale, most studies had conducted comparative studies of neighborhoods with different morphological characteristics for the correlation between urban morphology and pollutants [11,12] with air pollutant monitoring data from urban observatories. However, the specific relationship between urban morphological parameters and $PM_{2.5}$ concentration as well as diffusion has not been investigated clearly. In addition, the generalization of urban morphological characteristics needed a systematic and comprehensive framework. Since the selection of vegetation and non-physical morphological indicators is relatively weak in existing studies, they are unable to provide universal laws.

In recent years, the development of simulation techniques such as Computational Fluid Dynamics (CFD) has provided the technical support to establish the correlation between urban morphology and pollutant dispersion at the neighborhood scale with the Fluent simulation software being the most widely utilized. Studies could be divided into two categories. First, ideal-neighborhood simulation based on traditional settlement patterns [13] was constructed (lineal type, point group type, etc.). Different building combinations [14] or vegetation layouts [15] were explored individually, and the effect of different morphological features on the dispersion of pollutants based on simulation results was qualitative or quantitative analyzed. Secondly, a simulation based on actual cases was constructed. Different urban design schemes for the same neighborhoods [16] or comparisons of different neighborhoods [17] have been studied to promote the air quality. In general, the correlation between urban morphology and air quality had been gradually established; however, the quantitative guidance was limited. The simulation studies of ideal neighborhoods were separated from the complicated morphology of the building arrangement in the actual environment, and the simulation data were based on empirical data. In addition, in terms of modeling, the impact of the integrated neighborhood environment of buildings and vegetation on pollution dispersion has not been considered in previous studies, while the simulation studies of actual cases were aimed at promoting the air quality of specific public spaces and neighborhoods, which lacked the general application.

The study, which focused on two typical residential neighborhoods with different features in central Beijing, explored the quantitative rules of affection between urban morphology and air quality. We devised an urban morphology and air quality mechanism for selecting morphological parameters. Through the neighborhood-scale CFD simulation, which includes the calibration of vegetation factors and multi-source data, the Sensitive Morphological Parameters (SMPs) impacting air quality ($PM_{2.5}$, for example) at the neighborhood scale were filtrated before statistical models. Therefore, the quantitative rules of the influence of SMPs on the "pollutant-wind environment" could be estimated.

2. Data and Methods

2.1. Study Area

Taking a traditional residential area in central Beijing as the study area, the study selected a low-rise residential neighborhood (Neighborhood A) and a high-rise residential neighborhood (Neighborhood B) as the core study area based on the street network, buildings' layout, and its group form (Figure 1a). Neighborhood A, which was built in the 1990s, is dominated by enclosed low-medium-rise residential buildings with schools and underlying retail; Neighborhood B, which was built in the early twenty-first century, is dominated by row-slab high-rise residential buildings with a few underlying retails. The aforementioned two neighborhoods differ in terms of building periods, functional placement, and spatial arrangement, which might illustrate the main features of Beijing's residential neighborhood morphology.

(**a**)   (**b**)
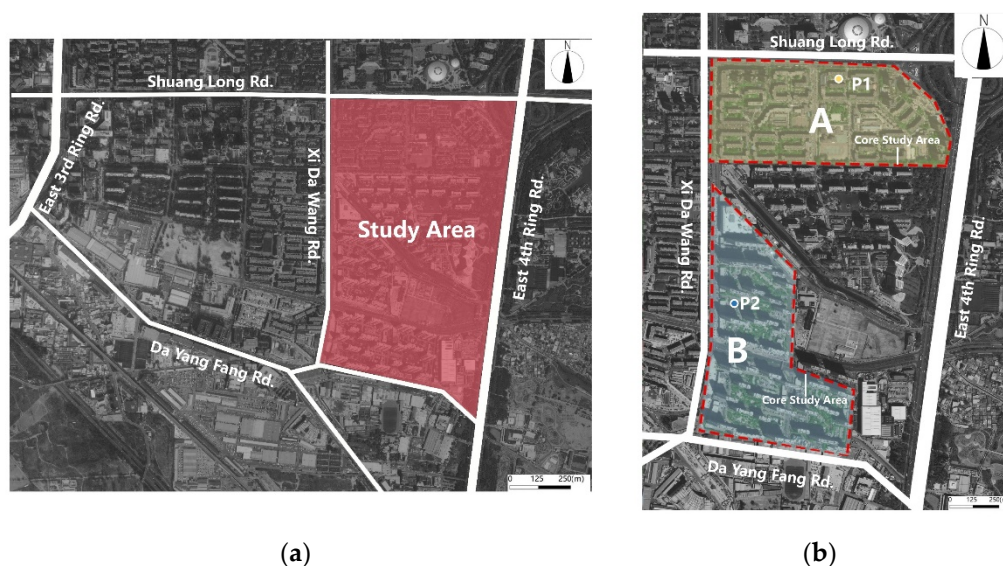
Figure 1. The study area: (**a**) the study area; (**b**) core study area, A refer to Neighborhood A, B refer to Neighborhood B.

### 2.2. Wind Environment and Pollutant Monitoring

The objective of the field monitoring is to count the concentration levels of pollutants in the neighborhoods as well as the characteristics of the wind environment and to conduct a preliminary analysis of the differences in pollutant concentrations and wind environment between neighborhoods, which serves as a foundation for testing and validating simulation results. The XL68 intelligent environmental monitoring equipment is chosen to monitor $PM_{2.5}$ concentration (resolution: 1 µg/m^3, range: 0~1000 µg/m^3) and wind speed (resolution: 0.1 m/s, range: 0~60 m/s) of the neighborhoods at monitoring points P1 and P2 (z = 3 m, z = 2 m) (Figure 1b). Details of equipment are shown in Table S1.

2.3. "Pollutant-Wind Environment" Model Setting

Micro-scale CFD numerical simulations have been widely used in the simulation of outdoor wind environments and pollutant dispersion [17]. ANSYS FLUENT 21.0 based on the finite volume method was adopted for numerical simulations, and the governing equation was the Reynolds-averaged Navier–Stokes equation. The standard K-ε turbulence model was adopted to simulate the airflow [18]. Pollutants and air were considered as continuous phases, and the pollutant concentrations were solved with the component transport model [19,20].

2.3.1. Computational Domain and Grid Generation

The calculation domain was constructed according to the method specified by the European Cooperation in the Field of Scientific and Technical Research (COST) [21], keeping a minimum of 5H for vertical distances (H—the maximum building height) and 5H for horizontal and horizontal distances (Figure 2). At the same time, an unstructured meshing method based on a hexahedron was adopted to save computational costs. Three sets of coarse–medium–fine meshes were divided, and grid irrelevance was tested. The final grid was 2.4×10^8 for Neighborhood A and 2.6×10^8 for Neighborhood B.

(**a**)   (**b**)
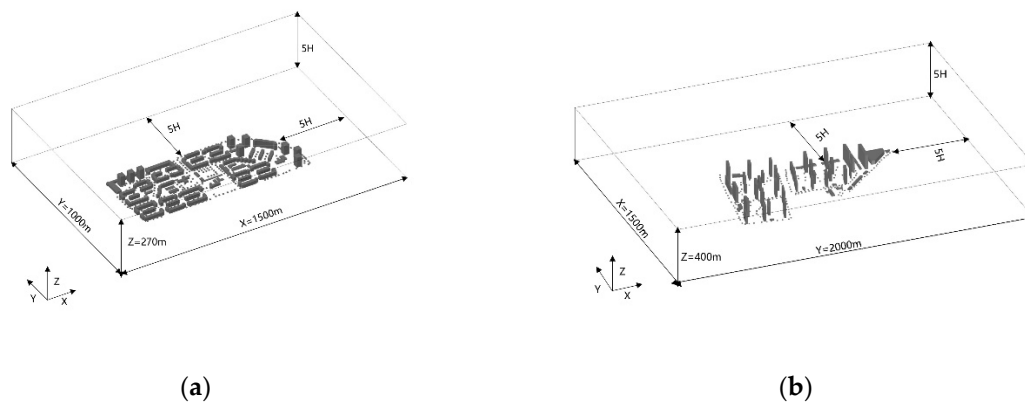
Figure 2. Computing domain construction of neighborhoods: (**a**) Neighborhood A; (**b**) Neighborhood B.
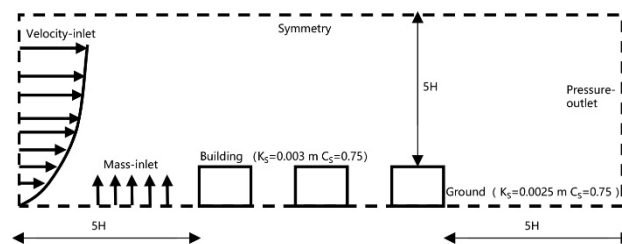
2.3.2. Boundary Condition

The incoming wind speed is exponentially distributed with height [22]. For the simulation, the calculation domain entry was set as the velocity-inlet boundary condition and adopted a user-defined function:

$$U = \frac{U_*}{\kappa} \ln\left(\frac{z + z_0}{z_0}\right) \tag{1}$$

U—horizontal wind speed at height z(m), m/s
U_*—ground friction speed, m/s
κ—Von·Karman constant, $\kappa = 0.42$
z_0—surface roughness, $z_0 = 0.25$

$PM_{2.5}$ was mainly emitted from traffic emissions and was relatively stable by default. Pollutants were emitted vertically upwards at 0.5 m/s, and the source intensity was from the nearest urban monitoring station on the simulation day. The zero static gauge pressure outlet was used for the downstream boundary condition, and the standard wall functions with roughness modification were used for the building surface and the bottom of the computational domain. The roughness height was 0.0025–0.003 m, and the roughness constant was 0.75. Symmetry boundary conditions were served to the side-face computational domain and the upper-face computational domain [23]. Detailed boundary conditions are shown in Figure 3.

Figure 3. Calculation of domain boundary condition settings.

The study treated the canopy section of the tree with a porous medium due to the influence of trees on the surrounding flow field in reducing wind speed and increasing flow disturbance. According to the relevant literature [24], the modeling of the influence of tree canopy on the flow field was accomplished by adding source terms to the momentum equation, the K equation and the ε equation, respectively. The porosity was 0.7, the inertial resistance was 0.18, and the viscous resistance was 1.67. Meanwhile, pollutant sorption

and deposition by trees were adjusted to a constant value, and the rate of deposition was determined by wind speed and pollutant concentration [25]:

$$Y_{PM2.5} = v \cdot d \cdot LAD \cdot t \tag{2}$$

$Y_{PM2.5}$—Pollutant adsorption capacity per unit area ($\mu g/m^2$)
v—Adsorption rate (m/s)
d—Pollutant concentration ($\mu g/m^3$)
LAD—leaf area density; (m^2/m^3)
t—Adsorption time (s)

2.3.3. Solution Settings

The finite volume method was used to discretize the control equation, solved by the SIMPLE algorithm, and the second-order upwind algorithm was adopted. In the initial condition setting, the ground observation data of the Beijing meteorological station on typical dates (Table 1) were used as the initial conditions for the simulation. $PM_{2.5}$ monitoring concentrations close to those of national control stations were used as the basis for selecting typical dates, and four typical dates with typical meteorological characteristics during the monitoring period were selected to establish the CFD numerical model.

Table 1. Meteorological data of national control stations on simulation dates.

Date	Wind Direction	Wind Speed (m/s)	$PM_{2.5}$ ($\mu g/m^3$)	Temperature (°C)
7.10	E	2.0	44	24.6
7.13	SE	1.7	55	28.6
10.14	N	1.8	9	9.2
10.26	NW	1.6	30	8.8

2.4. Selection and Extraction of Urban Morphological Parameters

2.4.1. Selection of Urban Morphological Parameters

Based on the research framework of urban morphology influencing air pollutant transport (Figure 4) and the generalization of existing studies, a system of six categories of urban morphological characteristics, including size, density, function, structure, shape and immaterial morphological characteristics, were constructed.
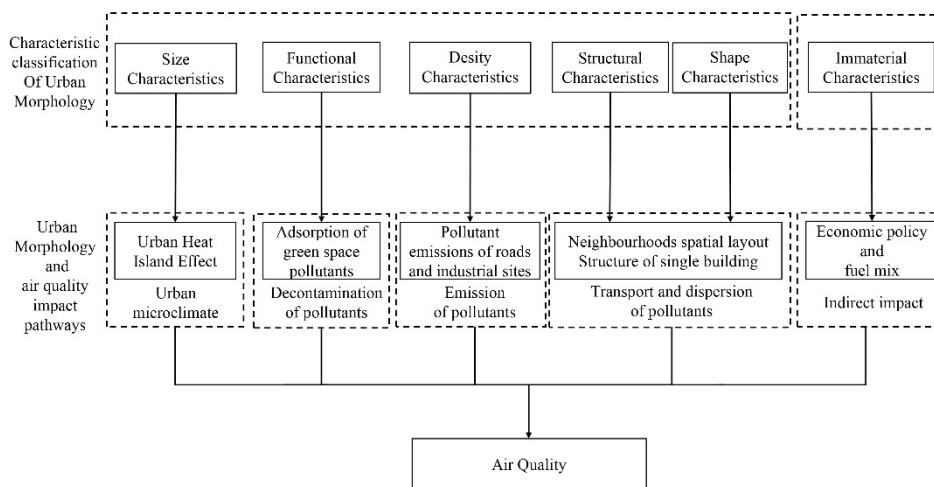
Figure 4. Framework of interaction mechanism between urban morphology and air quality.

The six morphological characteristics stated above have been proved to have a direct or indirect impact on air quality and the urban microclimate. In particular, urban size

affects the urban microclimate, pollutant emissions, and dispersion transport, and pollutant concentrations increase significantly as urban size increases [26]. The association between land use and air pollutants is more obvious, and air pollution is severe in industrial sites and commercial districts with greater emission sources [27]. In contrast, green spaces and water bodies can improve the local microclimate [28] and reduce the concentration of $PM_{2.5}$ in the region [29]. Different density characteristics demonstrate a broad range of heterogeneity in the routes of effect on air quality, such as the impact of building density on the alteration of local wind fields, which influences pollution dispersion [30,31], and the impact of road density on traffic pollutants [9]. Urban layout structure is a major factor affecting the wind environment, and a large number of scholars have conducted detailed studies on the elements of layout structure with wind environment and pollutant levels [32,33]. Most of the studies on shape features have focused on investigating the effects of different building shapes and combinations of building morphologies on the wind environment and pollutant dispersion [34]. Furthermore, since physical urban morphology is the spatial projection of non-physical urban morphology on land use [35], the adoption of the immaterial morphological indicator is highly relevant to the overall morphology of the neighborhoods.

Thus, ten morphological parameters were selected for investigation based on the principles of neighborhood scale, potential impact on pollutant levels, ease of implementation at the control and design stages, and the interaction mechanisms between the preceding morphological features and air quality, as well as the research progress of relevant literature (Table 2).

Table 2. Selection of characteristic morphological parameters of neighborhoods.

Morphological Characteristics	Morphological Parameters	Calculation Method
Size Characteristics	Total building area, TBA	$TBA = \sum_{i=1}^{n} S_i * F_i$ S_i—Building single-story area F_i— buildings Floors
	Floor area ratio, FAR	$FAR = TBA/SA$ SA—Neighborhoods area
Functional Characteristics	Greenbelt coverage rate, GCR	$GCR = TGA/SA$ TGA—Area of horizontal vegetation projection
Density Characteristics	Building density, BD	$BD = BBA/SA$ BBA—Building footprint
Structural Characteristics	Block envelope degree, BED	$BED = TBP/TSP$ TBP—Building envelope perimeter TSP—Neighborhood perimeter
	Space openness, SO	$SO = (1 - BD)/FAR$
Shape Characteristics	Average building volume, ABV	$ABV = \frac{\sum_{i=1}^{n} V_i}{n}$ V_i—Building volume
	Average building floors, ABF	$ABF = FAR/BD$
	The standard deviation of building height, SDH	$SDH = \sqrt{\frac{\sum_{i=1}^{n}(h_i - \bar{h})^2}{n}}$ $\bar{h}$—Average building height
Immaterial Characteristics	Population density, PD	$PD = TP/SA$ TP—Neighborhoods population

2.4.2. Extraction of Urban Morphological Parameters

The subject area's similarities and differences can be quantitatively investigated by the division of calculating units. The neighborhoods were divided into 20 units according to road boundaries, spatial structure divisions and the size of typical urban neighborhoods by a 200 × 200 m grid (Figure 5). The Beijing Institute of Surveying and Mapping was used to obtain the 3D environmental data of the neighborhoods, while the sociological data were

obtained from the field survey. The selected morphological parameters were calculated separately in ArcGIS 10.5.
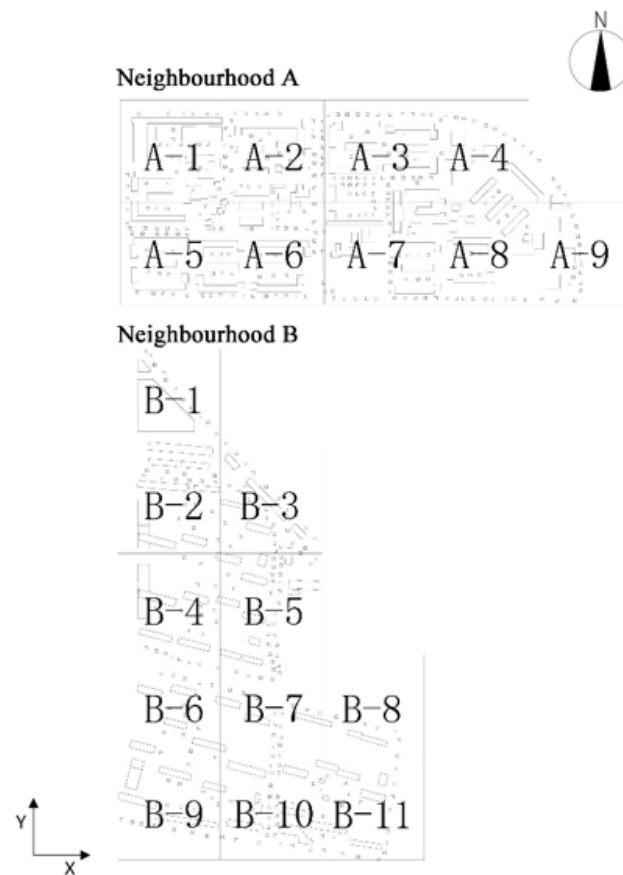
Figure 5. Grid division of neighborhoods.

2.5. Selection of Indicators for the Evaluation of "Pollutants–Wind Environment"

The "wind speed ratio" [23] evaluation index refers to the ratio of the wind speed at the actual selected location to the incoming wind speed on that day, which is often used to reflect the degree of influence of different areas or buildings on the wind speed, as a way to evaluate the condition of the wind environment in the region. "Pollutant concentration ratio" means the ratio of the concentration of pollutants in different areas to the concentration of incoming pollutants, which is used to quantify the relative level of pollution in a local area.

$$VR_w = \frac{V_p}{V_\infty} \qquad (3)$$

$$CR_p = \frac{C_p}{C_\infty} \qquad (4)$$

In Equations (3) and (4), VR_w is the wind speed ratio; V_p is the wind speed value at a certain height in a region (m/s); CR_p is the pollutant concentration ratio; V_p is the average concentration of pollutants at a certain height in a region ($\mu g/m^3$); V_∞ is the average concentration of incoming pollutants in a region ($\mu g/m^3$).

2.6. Statistic Analysis Model

The Pearson bivariate correlation analysis was used to filtrate the Sensitive Morphological Parameters (SMPs) with a high correlation to $PM_{2.5}$ and wind speed. To avoid the effect of excessive differences in the morphology of different neighborhoods, a correlation analysis was used between the GCR (A) in Neighborhood A and the GCR (B) in Neighborhood B separately.

The Curvilinear Regression was used to estimate the influence pattern of SMPs with $PM_{2.5}$ and wind speed. SMPs in 20 calculation units are used as independent variables, and the simulation results of the CR_p and VR_w at 1.5 m height are used as dependent variables.

3. Results

3.1. Monitoring Results

Field monitoring is shown in Figure 6. Overall, trends in pollutant concentrations within neighborhoods are influenced by overall urban background concentrations, and the two neighborhoods are relatively close but again show part of the local variability.
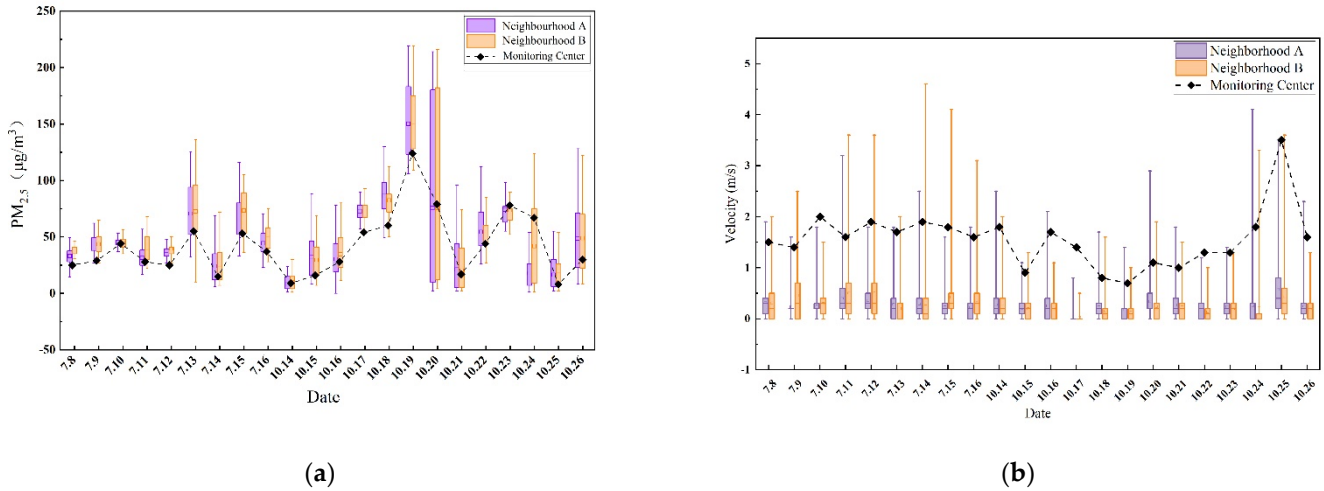
(a)　　　　　　　　　　　　　　　　　　　　　　　　**(b)**

Figure 6. Monitoring data: (**a**) $PM_{2.5}$ monitoring data; (**b**) wind speed monitoring data.

3.2. Simulation Results and Error Analysis

In the correlation test (Figure 7), the two data sets showed a high correlation (R^2 = 0.82, 0.77). In the paired *t*-test (Table 3), the data significance (P) was greater than 0.05 for both groups at 95% confidence, which means that there was no significant difference before and after the simulation.

As a result, the CFD numerical model developed can predict the neighborhoods' $PM_{2.5}$ concentration and wind environment more accurately. It can be used to predict a neighborhoods' $PM_{2.5}$ concentration and wind environment under different morphological parameters.
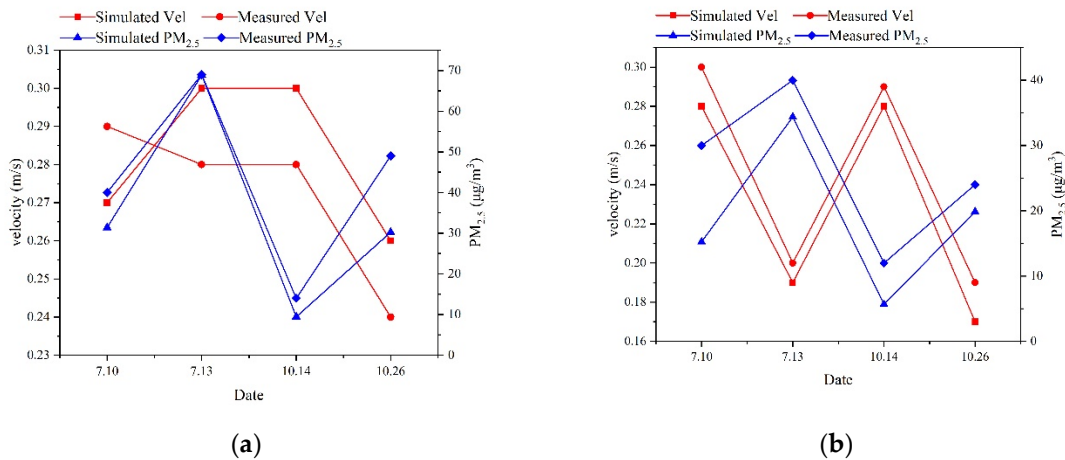
(a)　　　　　　　　　　　　　　　　　　　　　　　　**(b)**

Figure 7. Correlation test before and after simulation of: (**a**) Neighborhood A; (**b**) Neighborhood B.

Table 3. P1 and P2 simulated data were paired with measured data for the sample test.

| Comparing Criteria | Paired Differences | | | | | t | sig. (2-Tailed) |
| | Means | Std. Deviation | Std. Error Mean | 95% Confidence Interval of the Difference | | | |
				Lower	Upper		
Velocity	0.00875	0.026424	0.009342	−0.013341	0.030841	0.937	0.380
$PM_{2.5}$	8.27500	13.066615	4.619746	−2.648964	19.198964	1.79	0.116

3.3. Sensitive Morphological Parameters Filtrating

Table 4 shows the results of the correlation analysis between morphological parameters and the CR_p and VR_w of different neighborhoods. Among the 10 morphological parameters, BD, BED, ABV, ABF, SDH and GCR showed strong sensitivity ($p < 0.05$) to CR_p and VR_w with correlation coefficients between 0.4 and 0.8. It is suggested that there is a slight interaction between morphological parameters and pollutant concentrations and wind speeds, and alterations in these morphological parameters can result in more sensitive responses in $PM_{2.5}$ concentrations and wind conditions, which are Sensitive Morphological Parameters (SMPs). In contrast, the four parameters TBA, FAR, SO and PD were less sensitive ($p > 0.05$) to the $PM_{2.5}$ concentration ratio and wind speed ratio, with correlation coefficients below 0.3. It is suggested that alterations in these morphological features do not appear to produce more sensitive changes in $PM_{2.5}$ concentration and wind environment response.

Table 4. Correlation analysis of morphological parameters with $PM_{2.5}$ and wind speed.

| Analysis of Variables | CR_p | | VR_w | |
	R	P	R	P
TBA	−0.246	0.325	0.114	0.268
FAR	−0.246	0.325	0.114	0.268
BD	0.443	0.025	−0.709 **	0.000
SO	0.221	0.379	−0.217	0.388
BED	0.401	0.035	−0.636 **	0.001
ABV	−0.564 **	0.005	0.505 *	0.012
ABF	−0.628 **	0.002	0.684 **	0.000
SDH	−0.612 **	0.001	0.573 **	0.004
GCR (A)	−0.912 **	0.001	−0.818 **	0.007
GCR (B)	−0.726 **	0.001	−0.810 **	0.003
PD	0.162	0.520	−0.128	0.296

** The correlation is significant at the 0.01 level (two-tailed). * The correlation is significant at the 0.05 level (two-tailed).

Furthermore, the correlation coefficient R suggests that each SMP demonstrates an inverse trend of association between wind speed and $PM_{2.5}$. Among them, BD, BED and GCR show a positive correlation with $PM_{2.5}$ and a significant negative correlation with wind speed. ABV, ABF and SDH show part of negative correlation with $PM_{2.5}$ and a significant positive correlation with wind speed. Therefore, the SMPs influence the transport and dispersion of air pollutants primarily via altering the wind environment in the surrounding area: increased wind speed enhances the transport and dispersion of air pollutants, resulting in reduced air pollutant concentrations. In general, the wind environment is still the main factor influencing the dispersion of pollutants. In the case of identical neighborhoods' land uses, the different morphological parameters affect the dispersion of pollutants mainly indirectly by influencing the wind environment.

4. Discussion

4.1. Trend Analysis of the Influence of SMPs

Figure 8 shows the interaction curves of the six SMPs with $PM_{2.5}$ and wind speed. It also demonstrates that the effect of each SMP on $PM_{2.5}$ concentration and wind speed has an inverse connection within a particular interval, but the outcomes of other intervals on $PM_{2.5}$ concentration and wind speed are different.
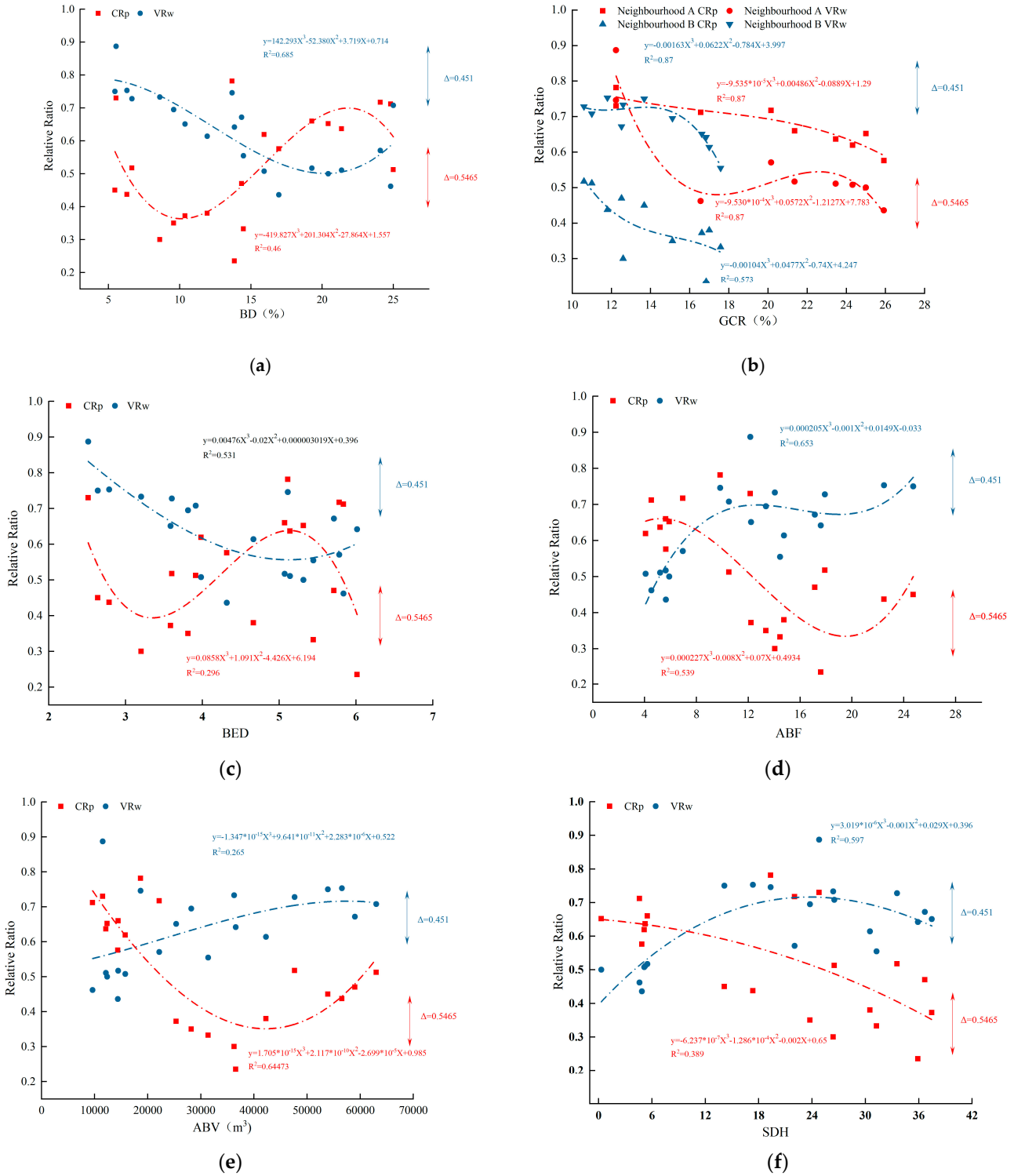
(**a**)

(**b**)

(**c**)

(**d**)

(**e**)

(**f**)

Figure 8. Curve fitting of different morphological parameters with $PM_{2.5}$ and wind speed: (**a**) BD; (**b**) GCR; (**c**) BED; (**d**) ABF; (**e**) ABV; (**f**) SDH.

According to Figure 8, wind speed is the most important element influencing $PM_{2.5}$ dispersion, and high wind speeds promote pollution transport and dispersion. The spatial morphological characteristics of distinct neighborhoods define their internal wind environment under the same incoming wind speed conditions, which has an impact on the transport dispersion and concentration distribution of air pollutants. Furthermore, the different impact results are exhibited by the morphological parameters in different intervals. It is claimed that there are parameter intervals for each morphological parameter that are more positive (or less positive) to the transmission and dispersion of air contaminants.

4.1.1. BD and BED

The relationship between BD, BED and $PM_{2.5}$ and wind speed all show a trend of sine and cosine curves (Figure 8a,c). As BD or BED rises, $PM_{2.5}$ shows a trend of decreasing, while wind speeds show a decrease followed by an increase, then increasing and then decreasing. In particular, $PM_{2.5}$ is lowest when BD is around 10% and continues to rise above 10%, reaching a maximum of $PM_{2.5}$ at around 20%. $PM_{2.5}$ is lowest at a BED of around 3 and highest at 5. When BD = 20% or BED = 5, the corresponding wind speed is at its minimum. The effect of BD and BED on the wind environment can be further seen by comparing the local area wind speed vectors for Neighborhood A and Neighborhood B (Figure 9): BD and BED of Neighborhood A with the relatively smooth internal wind environment is higher than Neighborhood B. This is because when the BD and BED are within a specific range, the transport of pollutants from outside is considerably restricted. However, when the BD and BED rise to a certain level, the neighborhood's wind environment tends to stabilize, which is not conducive to the migration and dispersion of atmospheric pollutants and creates a cumulative effect. Therefore, keeping the building density and block envelope degree of neighborhoods within a reasonable range can assist in enhancing air quality.
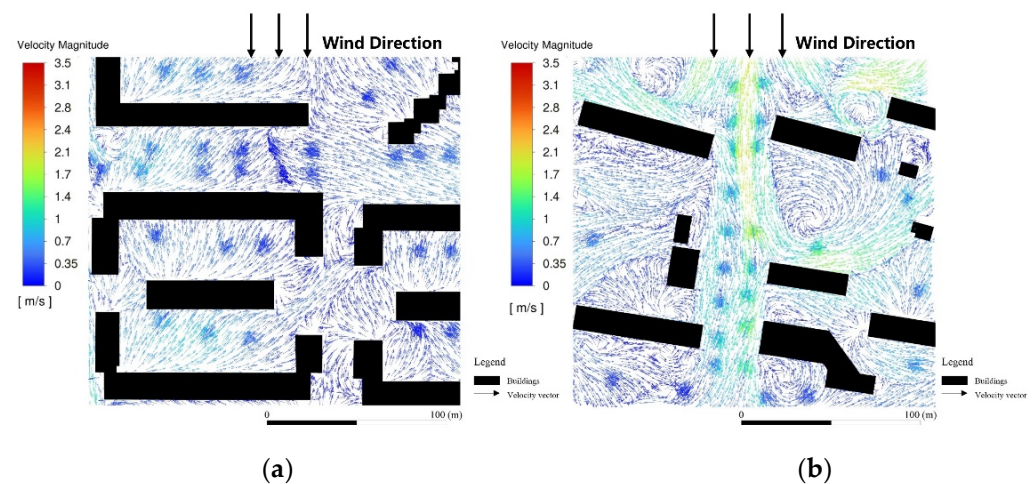
Figure 9. Vector diagram of local wind speed in: (**a**) Neighborhood A; (**b**) Neighborhood B.

4.1.2. GCR

As the GCR increases, $PM_{2.5}$ concentration and wind speed all showed a decreasing trend (Figure 8b). This is because wind speed is reduced and dust is suppressed by vegetation in the vertical zone beneath the canopy, with a progressive decrease in the zone above the canopy. As an example, Figure 10 illustrates the local vegetation XZ plane wind speed and $PM_{2.5}$ distribution in Neighborhood A, which suggests that the influence of vegetation on pollutant concentrations and wind speed is related to the height of the vegetation and its dust retention effect is most noticeable in the vertical zone beneath the canopy, with a progressive decrease in the zone above the canopy.

(**a**)

(**b**)
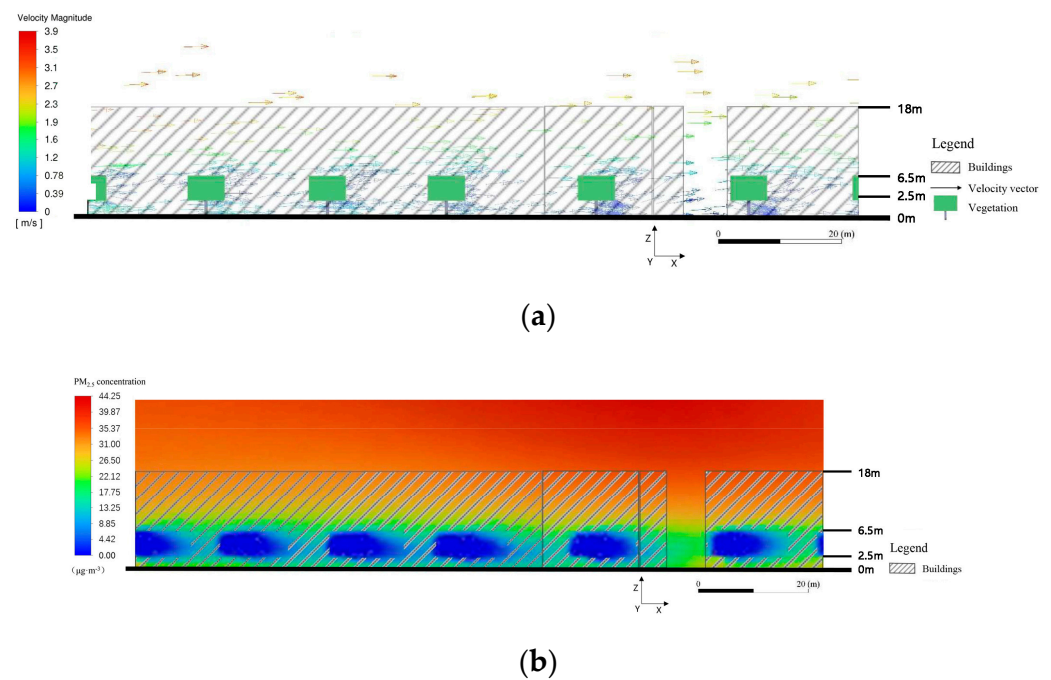
Figure 10. XZ plane in the local area of Neighborhood A of: (**a**) velocity vector; (**b**) $PM_{2.5}$ concentration distribution.

4.1.3. ABF, ABV and SDH

ABF, ABV and SDH demonstrated varying degrees of positive and negative correlations with $PM_{2.5}$ and wind speed, respectively. When ABV = 40,000 m^3 and ABF = 20F, the lowest $PM_{2.5}$ concentration was observed. The rise in ABF indirectly increases the building separation and enhances the air circulation within and outside the neighborhoods. When ABF exceeds 20, wind speed is further increased, but the static wind zone is formed on the leeward side of the building, which hinders the diffusion of pollutants (Figure 8d). As the ABV increases, $PM_{2.5}$ concentration shows a tendency to decrease and then increase (Figure 8e). This is because, within a certain volume range, increasing ABV helps to increase the open space and reduces the weakening effect on wind speed due to a large number of buildings. However, excessive ABV might increase the static wind area in the neighborhood and limit the effect of wind on pollution transmission.

The results reveal that the difference in height between buildings on the windward and leeward sides of the neighborhoods affects wind speed in the direction of incoming airflow differently (Figure 8f). Taking the example of four street valleys in the typical YZ plane of two neighborhoods (Figure 11), rising valley 1 and valley 4 are more effective in diffusing $PM_{2.5}$ in vertical space than falling valley 2 and valley 3. Therefore, reasonable SDH regulation promotes airflow rising, establishing a pleasant neighborhood wind environment, and boosting pollutant dispersion in vertical space. Moreover, angular flow zones are created with building heights up to a certain level, which enhances the dispersion of pollutants to the leeward side.
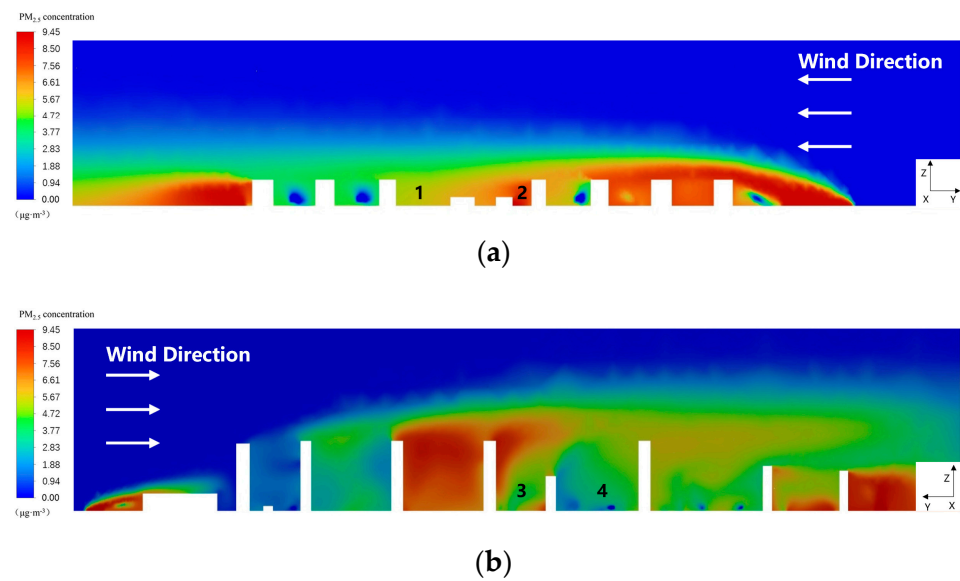
Figure 11. PM$_{2.5}$ diffusion distribution of typical Y-Z section in: (**a**) Neighborhood A; (**b**) Neighborhood B.

4.2. Morphology-Optimization Strategies for Pollutant Dispersion at Neighborhood-Scale

Based on the findings of the preceding investigation, strategies for optimizing neighborhood morphology based on air quality improvements were proposed. First, the relationship between BD, BED and PM$_{2.5}$ show a trend of sine and cosine curves. Therefore, BD should be reasonably controlled in the neighborhoods, and the BED of residential buildings along the street should be reduced while increasing the commercial buildings along the street (Figure 12a). Second, in terms of functional morphological characteristics, GCR showed a reduced influence on wind speed and PM$_{2.5}$ below the canopy, and the reducing effect decreases as the vertical height above the canopy increases. Therefore, it is critical to plant a diverse variety of vegetation species of varying heights (Figure 12b). Furthermore, it is important to increase the GCR while ensuring the functional integrity of the neighborhoods. Third, in terms of the shape morphological characteristics, ABF and ABV showed a trend of increasing and then decreasing with PM$_{2.5}$ values. Therefore, when the intensity of development is identified, specific buildings' heights should be increased, and the individual building's masses and number of total buildings in the neighborhood should be limited (Figure 12c). Additionally, the difference of building heights should be reasonably delineated (Figure 12d), according to the SDH curve fitting, to promote the climbing of incoming winds.
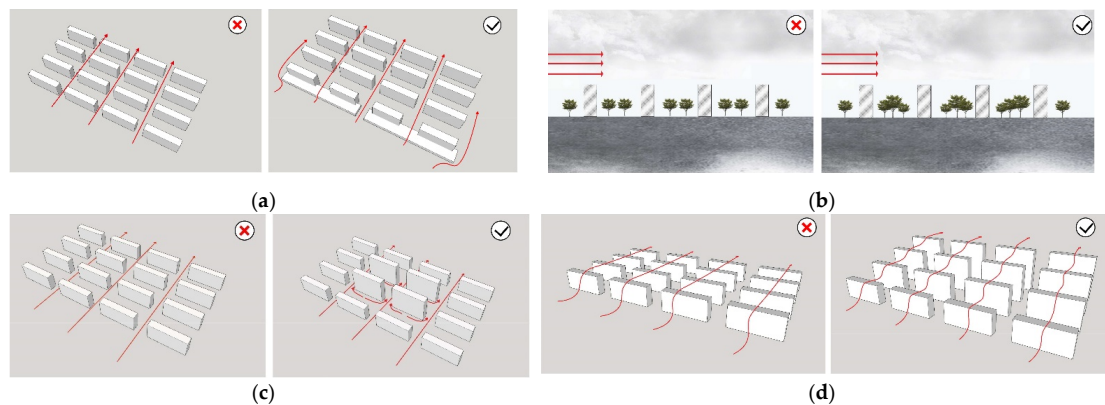
Figure 12. Morphology-optimization strategies for pollutant dispersion: (**a**) BED solution; (**b**) GCR solution; (**c**) ABV solution; (**d**) SDH solution.

5. Conclusions

This study aims to investigate the mechanisms underlying the correlation between urban form and atmospheric pollutants ($PM_{2.5}$, for example), and two types of typical residential neighborhoods in Beijing were selected as the study area. Morphological parameters were selected according to the research pathway of urban morphology affecting air quality, and a sensitivity analysis of morphological parameters with $PM_{2.5}$ and wind speed was carried out through field monitoring and CFD numerical simulation.

In the sensitivity filtrating, six morphological parameters, such as BD, BED, etc., showed high sensitivity to $PM_{2.5}$ concentrations and wind speed within the neighborhood, which are called the Sensitive Morphological Parameters (SMPs). The different correlations of SMPs between $PM_{2.5}$ and wind speed were observed. This demonstrates the existence of a tripartite relationship between morphological characteristics, wind environment, and pollutant dispersion.

The SMPs showed different influent rules on the $PM_{2.5}$ diffusion. It revealed a positive and cosine curve trend of BD and BED with $PM_{2.5}$. $PM_{2.5}$ is lowest when BD is around 10% and BED around 3 and continues to rise when BD is above 10%, reaching a maximum of $PM_{2.5}$ when BD is at around 20% and BED is at 5. GCR was significant to dust retention along with vertical canopy height, with a most noticeable effect in the vertical zone beneath the canopy and a progressive decrease in the zone above the canopy. When ABV = 40,000 m^3 and ABF = 20F, the lowest $PM_{2.5}$ concentration was observed. Increased SDH could promote airflow and enhance the capacity of $PM_{2.5}$ diffusion.

To optimize the circumstances of pollutant dispersion, three residential planning strategies were proposed. First, the BED of residential buildings along the street should be minimized while commercial buildings along the street should be expanded, and BD should be reasonably managed. Second, vegetation species of appropriate height should be considered, and GCR should be increased. Third, building height should be increased appropriately, as should a proper division of building height disparities in neighborhoods. Furthermore, acceptable control of individual building mass and the total number of buildings in the neighborhood should be considered.

References

1. *Beijing Ecological and Environmental Status Bulletin 2020*; Beijing Municipal Bureau of Ecology and Environment: Beijing, China, 2020.
2. Tao, Y.; Zhang, Z.; Ou, W. How does urban form influence $PM_{2.5}$ concentrations: Insights from 350 different-sized cities in the rapidly urbanizing Yangtze River Delta region of China, 1998–2015. *Cities* **2020**, *98*, 102581. [CrossRef]
3. McCarty, J.; Kaza, N. Urban form and air quality in the United States. *Landsc. Urban Plan.* **2015**, *139*, 168–179. [CrossRef]
4. Ding, W.; Hu, Y.; Dou, P. Study on the correlation between urban form and urban microclimate. *J. Archit.* **2012**, *7*, 16–21.

5.   Chen, M.; Dai, F. PCA-Based Identification of Built Environment Factors Reducing PM$_{2.5}$ Pollution in Neighborhoods of Five Chinese Megacities. *Atmosphere* **2022**, *13*, 115.

6.   Viecco, M.; Jorquera, H.; Sharma, A. Green roofs and green walls layouts for improved urban air quality by mitigating particulate matter. *Build. Environ.* **2021**, *204*, 108–120. [CrossRef]

7.   Wang, S.; Wang, J.; Fang, C. Estimating the impacts of urban form on CO$_2$ emission efficiency in the Pearl River Delta, China. *Cities* **2019**, *85*, 117–129. [CrossRef]

8.   Moradpour, M.; Hosseini, V. An investigation into the effects of green space on air quality of an urban area using CFD modeling. *Urban Clim.* **2020**, *34*, 100686. [CrossRef]

9.   Lee, C. Impacts of multi-scale urban form on PM$_{2.5}$ concentrations using continuous surface estimates with high-resolution in U.S. metropolitan areas. *Landsc. Urban Plan.* **2020**, *204*, 103935. [CrossRef]

10.   Hx, A.; Hong, C. Impact of urban morphology on the spatial and temporal distribution of PM$_{2.5}$ concentration: A numerical simulation with WRF/CMAQ model in Wuhan, China. *J. Environ. Manag.* **2021**, *290*, 112427.

11.   Dai, F.; Chen, M.; Wang, M.; Zhu, S.; Fu, F. Effect of Urban Block Form on Reducing Particulate Matter: A Case Study of Wuhan. *Chin. Landsc. Archit.* **2020**, *36*, 109–114.

12.   Cao, Q.; Luan, Q.; Liu, Y. The effects of 2D and 3D building morphology on urban environments: A multi-scale analysis in the Beijing metropolitan region. *Build. Environ.* **2021**, *192*, 107635. [CrossRef]

13.   Silva, F.; Reis, N.C.; Santos, J.M. Influence of urban form on air quality: The combined effect of block typology and urban planning indices on city breathability. *Sci. Total Environ.* **2022**, *814*, 152670. [CrossRef]

14.   Chao, Y.; Ng, E.; Norford, L.K. Improving air quality in high-density cities by understanding the relationship between air pollutant dispersion and urban morphologies. *Build. Environ.* **2014**, *71*, 245–258.

15.   Opa, B.; Pm, A.; Cc, A. Impact of morphological parameters on urban ventilation in compact cities: The case of the Tuscolano-Don Bosco district in Rome. *Sci. Total Environ.* **2022**, *807*, 150490.

16.   Yan, L.; Hu, W.; Gu, L. Correlation analysis between air quality in squares and spatial design elements: A case study on six design schemes of Urumqi diamond city square. *Urban Plan.* **2020**, *44*, 61–70.

17.   Hassan, A.M.; ELMokadem, A.A.; Megahed, N.A.; Eleinen, O.M.A. Urban morphology as a passive strategy in promoting outdoor air quality. *J. Build. Eng.* **2020**, *29*, 101204. [CrossRef]

18.   Li, Q.; Cai, X.; Kang, L. CFD simulations of flow and dispersion under construction disturbance conditions. *Res. Environ. Sci.* **2013**, *26*, 829–837.

19.   Wang, J.; Mu, Y. Study on spatial strategy responding to automobile exhaust pollution in urban street cantons. *Urban Plan.* **2013**, *37*, 54–60.

20.   Li, S.; Shi, T.; Zhou, S.; Gong, J.; Zhu, L.; Zhou, Y. Diffusion effects of atmospheric pollutants on the three dimensional landscape pattern of urban block. *J. Shenyang Jianzhu Univ. Nat. Sci.* **2016**, *32*, 1111–1121.

21.   Franke, J.; Hellsten, A.; Schlunzen, K.H. The COST 732 Best Practice Guideline for CFD simulation of flows in the urban environment: A summary. *Int. J. Environ. Pollut.* **2011**, *44*, 419–427. [CrossRef]

22.   Richards, P.J.; Norris, S.E. Appropriate boundary conditions for computational wind engineering models revisited. *J. Wind Eng. Ind. Aerodyn.* **2011**, *99*, 257–266. [CrossRef]

23.   Jiang, Z.; Cheng, H.; Zhang, P.; Kang, T. Influence of urban morphological parameters on the distribution and diffusion of air pollutants: A case study in China. *J. Environ. Sci.* **2021**, *105*, 163–172. [CrossRef] [PubMed]

24.   Li, L.; Li, X.; Lin, B.; Zhu, Y. Simulation of canopy flows using k-ε two-equation turbulence model with source/sink terms. *J. Qing Hua Univ. Nat. Sci.* **2006**, *4*, 753–756.

25.   Liu, W.; Yu, Z. Simulation on PM$_{2.5}$ detention service of green space in Haidian District, Beijing, China. *Chin. J. Appl. Ecol.* **2016**, *27*, 2580–2586.

26.   Zhang, S.; Han, L.; Zhou, W.; Li, W. Impact of urban population on concentrations of nitrogen dioxide (NO$_2$) and fine particles (PM$_{2.5}$) in China. *Acta Ecol. Sin.* **2016**, *36*, 5049–5057.

27.   Gao, Y.; Wang, Z.; Liu, C.; Peng, Z. Assessing neighborhood air pollution exposure and its relationship with the urban form. *Build. Environ.* **2019**, *155*, 15–24. [CrossRef]

28.   Wang, Y.; Akbari, H. A simulation study of the effects of street tree planting on Urban Heat Island mitigation in Montreal. In Proceedings of the 21st Canadian Connective Tissue Conference 2015, Quebec, QC, Canada, 28–30 May 2015.

29.   Dai, F.; Deng, Y.; Chen, M.; Guo, X. Effects of Green Space Layout on PM$_{2.5}$ in Different Types of Residential Areas Based on ENVI-met Simulation. *Landsc. Archit.* **2021**, *28*, 70–76.

30.   Yang, J.; Shi, B.; Shi, Y. Air pollution dispersal in high-density urban areas: Research on the triadic relation of wind, air pollution, and urban form. *Sustain. Cities Soc.* **2019**, *54*, 101941. [CrossRef]

31.   Aldegunde, J.A.Á.; Sánchez, A.F.; Saba, M.; Bolaños, E.Q.; Palenque, J.Ú. Analysis of PM$_{2.5}$ and Meteorological Variables Using Enhanced Geospatial Techniques in Developing Countries: A Case Study of Cartagena de Indias City (Colombia). *Atmosphere* **2022**, *13*, 506. [CrossRef]

32.   Adolphe, L. A simplified model of urban morphology: Application to an analysis of the environmental performance of cities. *Environ. Plan. B Plan. Des.* **2001**, *28*, 183–200. [CrossRef]

33.   Yang, J.; Zhang, T.; Fu, X. *Couping Mechanism between Wind Environment and Space form and Optimization Design in City Center*, 1st ed.; Southeast University Press: Nanjing, China, 2016; pp. 126–151.

34. Cheng, H.; Jiang, Z.; Zhang, P.; Kang, T. The influence of urban form parameters on the diffusion of air pollutant in residential area based on the CFD simulation. *J. Beijing Univ. Technol.* **2021**, *47*, 1377–1387.
35. Zhuang, Y.; Lu, J.; Chen, J. Exploring the "Morphological Structure" in contemporary urban design practices. *Archit. J.* **2021**, *5*, 91–98.